Roles of the atmosphere and ocean in the projected north atlantic warming hole

Qiuxian Li[1,2] · Yiyong Luo[1,2] · Jian Lu[3] · Fukai Liu[1,2] · Heli Teng[4]

Abstract
There exists a warming deficit in sea surface temperatures (SST) over the subpolar North Atlantic in response to quadrupled CO_2, referred to as the projected North Atlantic warming hole (WH). This study employs a partial coupling technique to accurately verify the relative roles of oceanic and atmospheric processes in the formation of the projected WH within an atmosphere-ocean coupled framework. By decomposing the SST anomalies in the subpolar North Atlantic into two components: those induced by atmospheric processes (i.e., the atmosphere-forced component) and those driven by changes in ocean circulation (i.e., the ocean-driven component), we find that the projected WH is primarily driven by changes in ocean circulation, with almost no contribution from atmospheric processes. Specifically, the slowdown of the Atlantic Meridional Overturning Circulation (AMOC) results in a cooling of SST in the WH region due to reduced northward ocean heat transport into this region. This study further quantifies the influence of a positive coupled feedback through surface heat flux (SHF) on the AMOC response under greenhouse gas forcing within this self-consistent framework. It is found that the AMOC slowdown leads to a negative SST anomaly in the subpolar North Atlantic and subsequently a positive ocean-driven SHF anomaly, which in turn further weakens the AMOC. This positive feedback through the SHF contributes about 50% to the total AMOC slowdown in response to quadrupled CO_2.

Keywords Sea surface temperature · North atlantic warming hole · Atlantic meridional overturning circulation · Surface heat flux

1 Introduction

Global sea surface temperature (SST) shows an overall warming trend due to increasing greenhouse gas concentrations since the industrial revolution (IPCC 2021). However, a pronounced lack of warming or even cooling has been observed in the subpolar North Atlantic SST over the past century (Drijfhout et al. 2012; Rahmstorf et al. 2015; He et al. 2022), known as the North Atlantic Warming Hole (WH). By analyzing results of climate models and observations, Chemke et al. (2020) have confirmed that the recent WH is of anthropogenic origin and related to ongoing greenhouse gas emissions. In addition, the North Atlantic WH is also present in future climate model simulations (Drijfhout et al. 2012; Winton et al. 2013; Marshall et al. 2015; Menery and Wood 2018; Keil et al. 2020). The presence of the WH has a wide range of potential effects on the climate of Europe and the Northern Hemisphere by altering atmospheric circulation (Gervais et al. 2016, 2019), such as affecting the North Atlantic storm track (Woollings et al. 2012) and surface pressure over Western Europe (Haarsma et al. 2015). Therefore, it is important to understand the physical mechanisms involved in the formation of the WH.

Many mechanisms are believed to be involved in the formation of the observed WH. However, the relative importance of ocean dynamics and atmospheric processes is still a topic of debate. For example, some model studies have suggested that the observed WH is caused by the slowdown of the Atlantic Meridional Overturning Circulation (AMOC) (Drijfhout et al. 2012; Rahmstorf et al. 2015; Caesar et al. 2018), while others have emphasized the significant role of atmospheric processes in the formation of the WH during the past century (Li et al. 2022a; He et al. 2022). Using an idealized ocean model forced by historical atmospheric forcing, Li et al. (2022a) found that about 54%

National Satellite Ocean Application Service, Beijing, China

Yiyong Luo yiyongluo@ouc.edu.cn

1 Frontier Science Center for Deep Ocean Multispheres and Earth System (FDOMES) and Physical Oceanography Laboratory, Ocean University of China, Qingdao, China

2 College of Oceanic and Atmospheric Sciences, Ocean University of China, Qingdao, China

3 Atmospheric Sciences and Global Change Division, Pacific Northwest National Laboratory, Richland, WA, USA

4

of the observed cooling trend in the subpolar North Atlantic SST can be attributed to increased ocean heat loss caused by local atmospheric forcing. He et al. (2022) reached a similar conclusion using a slab ocean model. They found that about 50% of the observed cooling trend can be attributed to enhanced ocean heat loss resulting from increased local westerly winds in the subpolar North Atlantic. Moreover, increased warming in the Indian Ocean drives an increase in local precipitation, which, through teleconnection, strengthens the westerly winds south of Greenland, which in turn cools the SST over the North Atlantic subpolar region through heat flux (Hu and Fedorov 2020). On the other hand, anthropogenic aerosol forcing has been found to hinder the formation of the WH and delay the appearance of the WH by about 30 years (Dagan et al. 2020).

However, for the projected WH under future warming scenarios, there seems to be a general consensus on the dominant role of oceanic processes (especially the slowdown of the AMOC) (Drijfhout et al. 2012; Woollings et al. 2012; Rugenstein et al. 2013; Winton et al. 2013; Marshall et al. 2015; Gervais et al. 2018; Menary and Wood 2018; Chemke et al. 2020; Keil et al. 2020; Liu et al. 2020; Ren and Liu 2021). For example, by comparing the results of a slab ocean model with those of a fully coupled model under greenhouse gas forcing, Woollings et al. (2012) found that the WH disappears in the slab ocean model but persists in the corresponding fully coupled model, confirming the dominant role of oceanic processes in the projected WH. Similarly, by comparing a pair of fully coupled simulations with and without ocean circulation changes, Winton et al. (2013) found that the WH disappears when changes in ocean circulation are suppressed, verifying that ocean circulation changes are critical to the generation of the projected WH. In addition, by employing passive tracers within an ocean-only framework, Marshall et al. (2015) concluded that changes in ocean circulation are important for the SST response in the North Atlantic. Furthermore, through heat budget analysis, Menary and Wood (2018) found that the formation of the WH is related to changes in ocean heat transport associated with changes in ocean circulation. More recently, Keil et al. (2020) found that the WH in a forced scenario is influenced by changes in ocean heat transport associated with both overturning and gyre circulation changes. Using a sensitivity experiment that stabilizes the AMOC strength in an anthropogenic warming climate, Liu et al. (2020) found that the WH disappears without an AMOC slowdown, suggesting that the AMOC slowdown is the primary cause of the future WH. However, these previous studies have used either idealized models (Woollings et al. 2012; Winton et al. 2013; Marshall et al. 2015; Liu et al. 2020) or statistical analyses and diagnostic methods (Drijfhout et al. 2012; Kim and An 2013; Rugenstein et al. 2013; Gervais et al. 2018; Menary and Wood 2018; Keil et al. 2020) to determine the importance of changes in ocean circulation in the formation of the projected WH. They have not been able to accurately disentangle the contributions of oceanic and atmospheric processes in the formation of the projected WH in an atmosphere-ocean coupled system. In summary, while previous studies have laid the groundwork for understanding the role of AMOC slowdown in the projected warming hole, our study provides a more comprehensive insight through the application of the partial coupling technique. The partial coupling technique is in the spirit of the fixed circulation experiments of Winton et al. (2013) and Liu et al. (2020), both of which suppress the effect of ocean circulation changes on the air-sea interaction. However, these previous studies have not been able to accurately disentangle the contributions of oceanic and atmospheric processes in the formation of the projected WH in an atmosphere-ocean coupled system. In this study, we aim to better quantify the relative roles of oceanic and atmospheric processes in the formation of the WH under greenhouse gas forcing by precisely separating them, in particular to isolate the role of oceanic processes in the projected WH. To this end, we use a set of experiments in the Community Earth System Model (CESM) designed by Garuba et al. (2018), in which the anomalous SST can be decomposed into atmosphere-forced (i.e., forced by atmospheric processes) and ocean-driven (i.e., driven by changes in ocean circulation) components within a coupled framework. As will be shown later, the crucial role of the AMOC slowdown in the projected WH under greenhouse gas forcing is confirmed by the results of this novel decomposition method. The partially coupled framework used in this study allows for the isolation of both atmosphere- and ocean-driven temperature and surface heat flux anomalies as well as their associated climate feedbacks.

Another goal of the study is to quantify the effect of a positive coupled feedback through the surface heat flux (SHF) on the AMOC response under greenhouse gas forcing. In the atmosphere-ocean coupled system, a change in the ocean circulation initially caused by atmospheric forcing can feed back to change the SST, which can further affect the ocean circulation through the air-sea interaction, i.e., there is a coupled feedback (Garuba and Klinger 2016; Gregory et al. 2016). To improve our confidence in the future climate response projected by climate models, it is essential to understand the coupled feedback mechanism. In the North Atlantic, the coupled feedback is positive and acts to further increase the surface heat flux into the ocean and weaken the AMOC (Garuba and Klinger 2016; Gregory et al. 2016; Todd et al. 2020). Specifically, under greenhouse gas forcing, the warmer surface air temperature relative to the SST results in reduced heat loss from the ocean over the subpolar North Atlantic. This positive surface heat flux anomaly reduces surface density and induces a slowdown of the AMOC. Consequently, the weakened AMOC leads to

surface cooling of the subpolar North Atlantic SST (i.e., the WH) by reducing northward ocean heat transport. This cooling of the SST further decreases surface heat loss from the ocean, exacerbating the weakening of the AMOC. Attempts have been made to quantify the coupled feedback associated with the AMOC response using the Flux-Anomaly-Forced Model Intercomparison Project (FAFMIP) experiments (Gregory et al. 2016; Todd et al. 2020; Couldrey et al. 2023). In particular, by comparing the results of the FAFMIP experiments between the atmosphere-ocean coupled model and the ocean general circulation model (OGCM), both of which are forced by the surface heat flux anomalies computed from the CMIP5 ensemble 1pctCO_2 scenario, Todd et al. (2020) found that the AMOC weakening in the coupled experiments is on average 10% larger than that in the oceanonly experiments, attributing the 10% larger weakening to the positive feedback due to the ocean-atmosphere coupling. However, their experiments cannot unambiguously isolate the effect of the positive coupled feedback on the AMOC weakening because the prescribed surface heat flux perturbation applied in their OGCM experiments is derived from fully coupled systems in which the effect of the coupled feedback is already included. Therefore, the OGCM runs already contain the imprints of the atmosphere-ocean coupling, and the comparison between the coupled and OGCM experiments does not cleanly isolate the effect of the coupled feedback through SHF on the AMOC response. In this study, we investigate the role of the positive feedback through SHF on the AMOC response under greenhouse gas forcing in a cleaner and more consistent framework.

The model experiments for the separation of the atmosphere-forced and ocean-driven components are described in Model experiments. Response and mechanism of the WH presents the response and mechanism of the projected WH, as well as the relative contributions of atmospheric and oceanic processes. The effect of the positive feedback through the SHF on the AMOC weakening is analyzed in Positive feedback mechanism in AMOC response. Conclusion summarizes the main conclusions of this study.

Table 1 Model experiments with CESM1

Name	Run (yrs)	Description
CTRL	150	Control fully coupled simulation (Preindustrial CO_2)
FULL	150	Perturbed fully coupled simulation (4×CO_2)
PARTIAL	150	Perturbed partially coupled simulation (4×CO_2)

2 Model experiments

In the CESM-based experimental framework implemented by Garuba et al. (2018), three simulations (Table 1) are used to separate the atmosphere-forced component from the ocean-driven component: the control simulation (CTRL), the fully coupled simulation (FULL) and the partially coupled simulation (PARTIAL). All three simulations are initialized from a 1000-year preindustrial simulation in NCAR and integrated for 150 years. The CTRL is integrated with preindustrial CO_2 concentrations, while the FULL and PARTIAL are forced by abrupt CO_2 quadrupling. The main difference between the FULL and PARTIAL simulations is that the former uses the standard atmosphere-ocean coupling, while the latter suppresses the effect of ocean circulation changes on the atmosphere-ocean coupling through a partial coupling approach, which is explained as follows.

2.1 Surface-forced and dynamically induced component decomposition

We first review the tracer decomposition method commonly used in previous studies to isolate the role of changes in surface heat flux and ocean circulation on the ocean temperature response (Banks and Gregory 2006; Xie and Vallis 2012; Bouttes et al. 2014; Gregory et al. 2016; Garuba and Klinger 2016). The change of ocean temperature response to external forcing (T'_{OF}) can be expressed as:

$$\frac{DT'_{OF}}{Dt} = Q' - v'_F \cdot \nabla \bar{T} \tag{1}$$

where Q is the surface heat flux anomaly due to the external forcing; $\boldsymbol{v}'_F$ is the three-dimensional ocean circulation anomalies in response to the external forcing; $\bar{T}$ represent the control value of the ocean temperature; D/Dt is the total derivative ($D/Dt = \partial/\partial t + v \bullet \nabla$); subscript F denotes the variables in the fully coupled experiment. Equation (1) indicates the total response of ocean temperature is caused by both the change in surface heat flux (Q) and the

$$\frac{DT'_{FS}}{Dt} = Q'$$

$$\frac{DT'_{FD}}{Dt} = -v'_F \cdot \nabla \bar{T} \tag{2}$$

(3)

The T'_{FS} and T'_{FD} are known as surface-forced component and dynamically induced component, respectively. In practice, two additional temperature-like tracers (Banks and Gregory 2006; Xie and Vallis 2012) are introduced in order to obtain T'_{FS} and T'_{FD}.

However, the above decomposition does not cleanly isolate the ocean-driven component from the atmosphereforced one. To explain the air-sea interaction conceptually, the surface heat flux anomaly can be thought of as related to the air-sea temperature difference:

$$Q' = \alpha \left(T'_{AF} - T'_{OF}\right)|_s = \alpha \left(T'_{AF} - T'_{FS} - T'_{FD}\right)|_s \tag{4}$$

where T'_{AF} is the atmospheric temperature anomaly; $|_s$ represents surface values of the variables; α represents the strength of the coupling between the atmosphere and ocean. Equation (4) has been confirmed to be a good approximation of the bulk formula that is actually used in computing the turbulent surface flux exchange (Haney 1971; Rahmstorf and Willebrand 1995). The actual calculation of the surface heat flux is done through the bulk formula provided by the coupler of the CESM modeling framework. Equation (4) shows that the change in surface heat flux (Q) itself is partly dependent on the SST change induced by ocean circulation changes (T'_{FD}) and the surface air temperature change coupled with the T'_{FD}. Therefore, the T'_{FS} component that forced by the surface heat flux change (Q) is also influenced by the changes in ocean circulation and is not exclusively originating from the atmosphere. Given this shortcoming, a cleaner decomposition method needs to be developed to separate the ocean-driven component (T'_{OO}) from the purely atmosphere-forced component (T'_{OA}) of the ocean temperature response. Meanwhile, the surface heat flux anomaly (Q) need to be decomposed into two components: the atmosphere-forced component (Q'_A) triggered directly by the increased atmospheric CO_2 and the oceandriven changes in ocean circulation, which advect the control ocean temperature field ($v'_F \bullet \nabla \bar{T}$). Thus, we can partition the T'_{OF} into two parts based on these forcings: component (Q'_O) caused indirectly by changes in ocean circulation, i.e., $Q' = Q'_A + Q'_O$.

2.2 Atmosphere-forced and ocean-driven component decomposition

The crucial step in isolating the temperature response that is solely attributed to atmospheric forcing is to eliminate the ocean-driven component (Q'_O) from the surface heat flux anomaly. To this end, in the partially coupled simulation, a passive tracer T'_{PS} is introduced, which is similar to T'_{FS} but only responds to the atmosphere-forced component of the surface heat flux anomaly (Q'_A). Then, this surface-forced temperature component T'_{PS} instead of the total ocean temperature T'_{OF} is used to couple with the atmosphere to avoid the influence of the ocean dynamically induced temperature T'_{FD} on the surface fluxes. This partial coupling achieves a better consistency between the surface heat flux anomaly originating from the atmosphere (Q'_A) and the surface-forced ocean temperature tracer (T'_{PS}) in the partially coupled simulation. This relationship can be formulated as follows:

$$\frac{DT'_{PS}}{Dt} = Q'_A \tag{5}$$

$$Q'_A = \alpha \left(T'_{AP} - T'_{PS}\right)|_s \tag{6}$$

where T'_{AP} is the atmospheric temperature anomaly, which is induced by CO_2 increase and coupled with the T'_{PS}. Hence, the surface-forced ocean temperature (T'_{PS}) in the partially coupled simulation is entirely of atmospheric origin and can be referred to as the purely atmosphere-forced component (T'_{OA}), which is governed by:

$$\frac{DT'_{OA}}{Dt} = Q'_A \tag{7}$$

Furthermore, the ocean-driven surface flux anomaly (Q'_O) induced by ocean circulation changes works together with the advection of the control ocean temperature field due to ocean circulation changes ($\boldsymbol{v}'_F \bullet \nabla \bar{T}$), governing the ocean-driven component of ocean temperature response, which evolves according to:

$$\frac{DT'_{oo}}{Dt} = Q'_O - \boldsymbol{v}'_F \cdot \nabla \bar{T} \tag{8}$$

It also can be derived from Eq. (1) minus Eq. (7).

In summary, we can cleanly separate the atmosphereforced component (i.e., Q'_A and T'_{OA}) from the ocean-driven component (i.e., Q'_O and T'_{OO}) with the help of the partial coupling technique. The atmosphere-forced components are obtained directly from the partially coupled experiment, while the ocean-driven components can be obtained as the differences between the fully coupled and the partially coupled simulation. The validity of the linear assumption that the ocean-driven component can be derived by subtracting the partially coupled simulation from the fully coupled simulation has been demonstrated by Garuba and Rasch (2020). Interested readers are referred to Garuba and Rasch (2020); Li et al. (2022b) for further technical details.

3 Response and mechanism of the WH

We first examine the temporal evolution of SST over the North Atlantic WH region and in the Northern Hemisphere (NH) in response to quadrupled CO_2. The WH region (45°W-10°W, 50°N-65°N) is defined as the area with the largest SST cooling in response to quadrupled CO_2. Results show that the SST changes in the WH region are consistently weaker than the NH average, and the SST in the WH region shows a negative anomaly after 50 years of model integration (Fig. 1), which is consistent with many previous studies (Marshall et al. 2015; Gervais et al. 2018; Menary and Wood 2018; Keil et al. 2020). Using the fully coupled and partially coupled experiments with the CESM (Table 1), the response of SST in the WH region can be decomposed

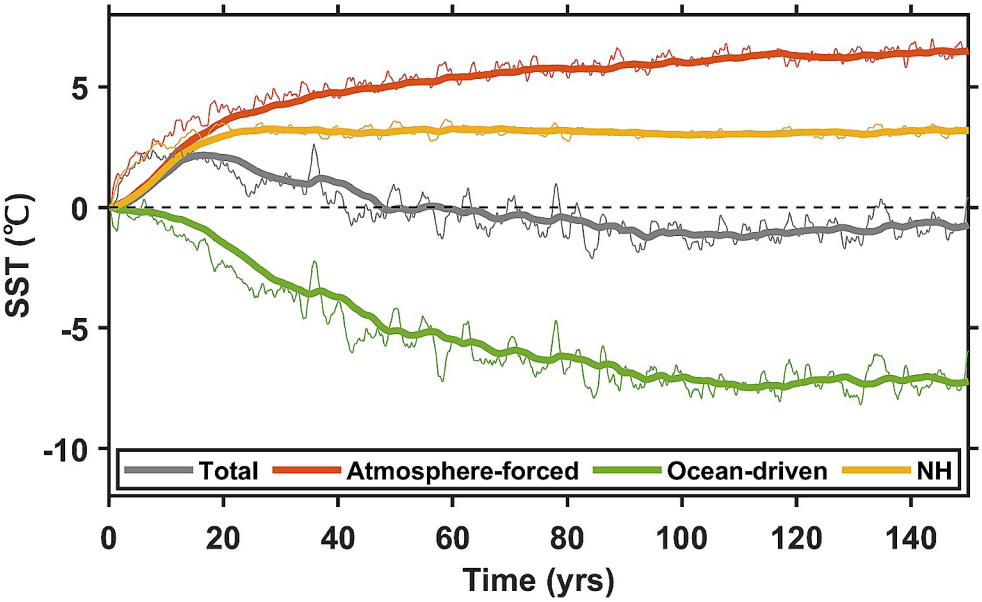

Fig. 1 Time series of the SST anomalies (°C) in the North Atlantic warming hole region (WH: 45°W-10°W, 50°N-65°N) in response to quadrupled CO_2: the total response (gray) and its atmosphere-forced (red) and ocean-driven (green) components. Superimposed yellow line is the time series of the mean SST anomaly in the North Hemisphere (NH). Thin lines show annual means; thick lines are smoothed over 11 years

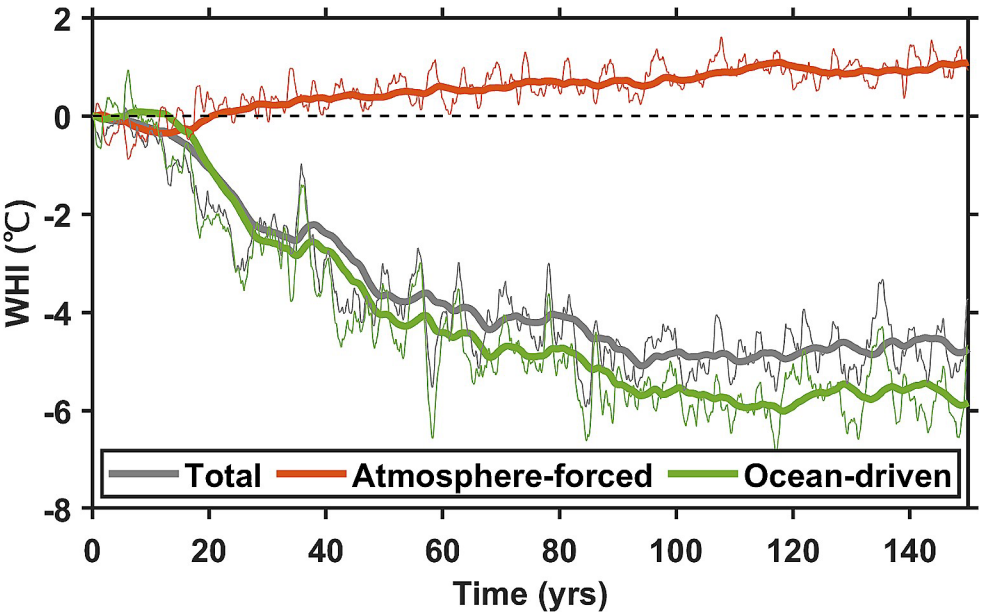

Fig. 2 Time series of warming hole index (WHI; °C) in response to quadrupled CO_2: the total response (gray) and its atmosphere-forced (red) and oceandriven (green) components. Thin lines show annual means; thick lines are smoothed over 11 years

into a component induced by atmospheric forcing and a component driven by ocean circulation changes. It is clear that the atmospheric forcing leads to a continuous warming of the SST in the WH region (red line in Fig. 1), while the effect of ocean circulation changes results in a cooling of the SST (green line in Fig. 1). During the first 40 years, the warming induced by the atmospheric forcing overwhelms the cooling resulted from the changes in ocean circulation, leading to a positive SST anomaly in the WH region. Subsequently, the negative SST anomaly induced by ocean circulation changes gradually becomes dominant.

To quantify the strength of the WH and the contributions from atmospheric and oceanic processes, we next examine the warming hole index (WHI), defined as the difference between the SST anomalies averaged in the WH region and the NH (Keil et al. 2020):

$$WHI = SST_{WH} - SST_{NH}$$

Here we consider the difference in SST instead of surface temperature to eliminate the effect of the land-ocean warming contrast. In addition, since the Southern Hemisphere SST shows a much weaker warming overall, which would suppress the WH signal, we use the Northern Hemisphere mean SST as a reference instead of the global mean SST.

Figure 2 shows the evolution of the WHI over time and the contribution of atmospheric and oceanic processes. It is found that the WHI is always negative (gray line in Fig. 2), indicating that the warming of SST in the WH region is consistently weaker than in the NH region. By decomposing the WHI into the atmosphere-forced component (red line in Fig. 2) and the ocean-driven component (green line in Fig. 2), we find that the atmospheric forcing leads to a positive WHI except during the first 15 years, when the atmospheric forcing results in stronger warming in the WH region than in the NH region. On the contrary, the ocean circulation changes always drive a negative WHI, and the evolution of the ocean-driven WHI satisfactorily explains the evolution of the total WHI. Therefore, the North Atlantic WH in response to quadrupled CO_2 is predominantly the result of changes in the ocean circulation, with almost no contribution from atmospheric processes. This is consistent with previous studies on the dominant role of ocean processes in the projected WH (Woollings et al. 2012; Rugenstein et al. 2013; Winton et al. 2013; Marshall et al. 2015; Gervais et al. 2018; Menary and Wood 2018; Chemke et al. 2020; Keil et al. 2020; Liu et al. 2020; Ren and Liu 2021). In addition, previous modeling studies have shown that the development of the projected WH is associated with a reduction in the northward ocean heat transport (OHT) due to the weakening of the AMOC (Drijfhout et al. 2012; Collins et al. 2013; Rahmstorf et al. 2015; Liu et al. 2020; Ren and Liu 2021).

We then proceed to verify the decisive role of AMOC weakening in the formation and temporal evolution of the projected WH under greenhouse gas forcing. Figure 3 shows the temporal evolution of changes in the AMOC strength, defined as the maximum streamfunction below 500 m at 45°N (Ma et al. 2021), and the changes in the OHT across the 50°N Atlantic (the southern boundary of WH region) in response to quadrupled CO_2. It can be seen that the AMOC strength weakens rapidly (blue line in Fig. 3), leading to a synchronous reduction in the northward OHT (red line in Fig. 3), which is consistent with previous studies (Gregory et al. 2005; Weaver et al. 2012; Cheng et al. 2013; Rahmstorf et al. 2015; Bakker et al. 2016; Wen et al. 2018; Weijer et al. 2020). A further analysis finds that both heat input to and export from the WH region decrease in response to quadrupled CO_2, with the decrease in the former being much larger than that in the latter (Fig. 4a). Therefore, it is the weakening of OHT across the southern boundary (50°N) that primarily contributes to the divergence of heat in the WH region. Moreover, approximately 78% of the decrease in OHT at 50°N is attributable to the overturning component of the OHT change (Fig. 4b), which is directly linked to the weakening of the AMOC. As expected, the changes in the AMOC strength and OHT correspond well with the

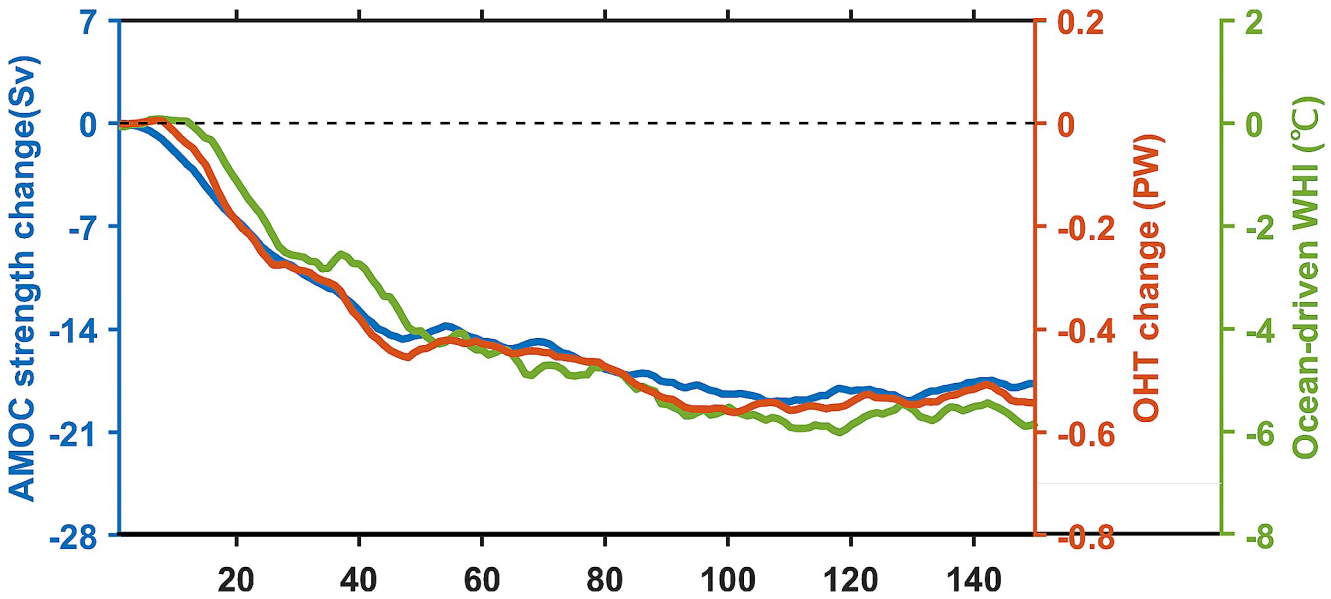

Fig. 3 Time series of the changes in AMOC strength (Sv; blue), the meridional ocean heat transport (OHT; PW; red) at 50°N of the Atlantic Ocean, and the ocean-driven WHI (°C; green) in response to quadrupled CO_2. All lines are smoothed over 11 years

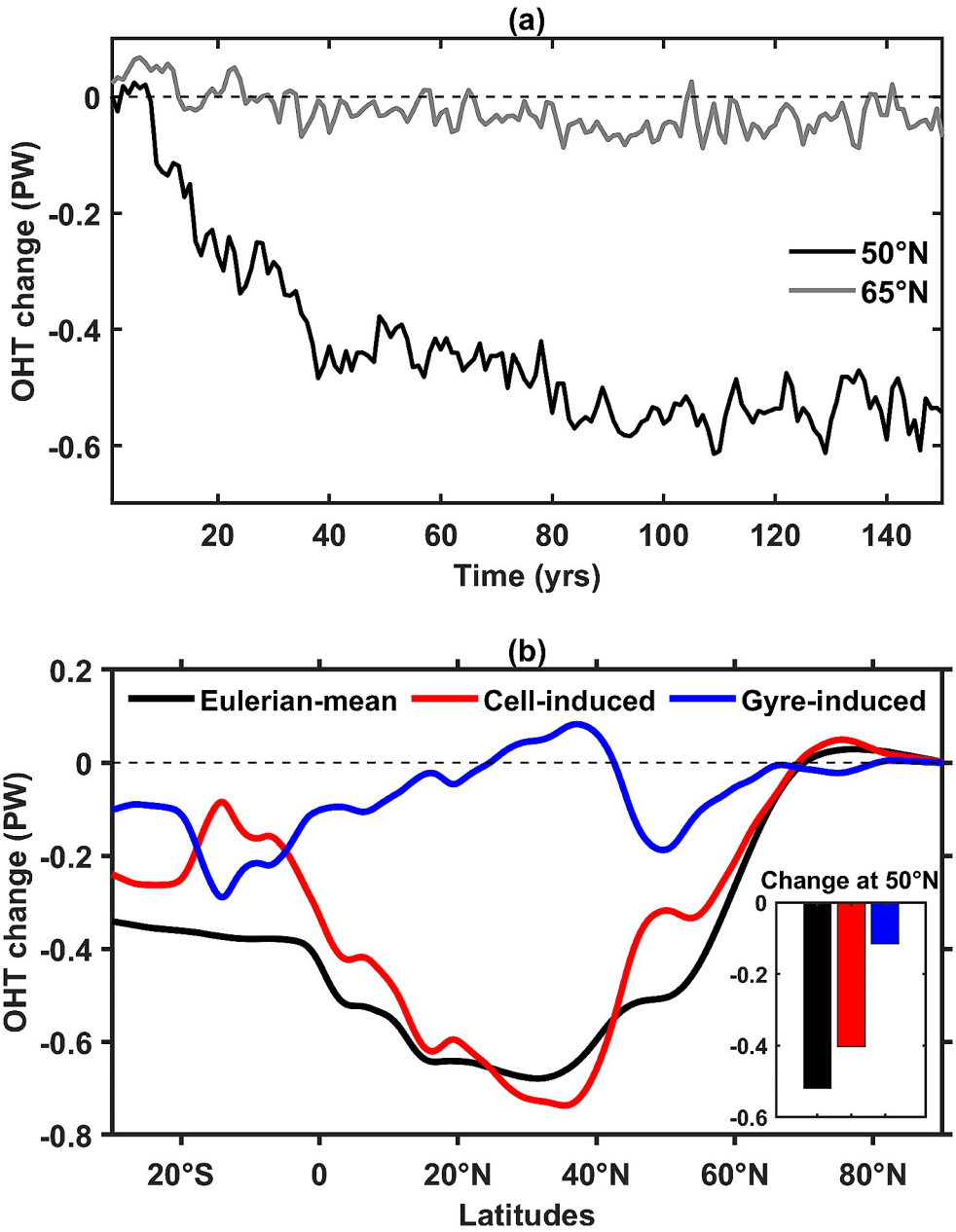

Fig. 4 (**a**) Time series of the meridional ocean heat transport anomalies (OHT; PW) at 50°N (black) and 65°N (gray) of the Atlantic Ocean. (**b**) Changes of the Eulerian-mean OHT (black) in response to quadrupled CO_2 as well as its cell-induced OHT (red) and gyre-induced OHT (blue) in the Atlantic Ocean. The bar graph shows the result at 50°N

temporal evolution of the ocean-driven WHI (green line in Fig. 3), confirming that the slowdown of the AMOC results in a deficit in warming or even cooling of the SST in the WH region by reducing the northward OHT.

Since the WHI reaches quasi-equilibrium after ~ 100 years of simulation (Fig. 2), a mean of years 101–150 is used for further analysis of the spatial pattern and mechanism of the North Atlantic WH. The results remain consistent regardless of the period chosen for analysis (not shown). Similar to the spatial patterns derived from previous climate models (Drijfhout et al. 2012; Menary and Wood 2018; Keil et al. 2020), the response of SST in the North Atlantic shows a cooling in the northern subpolar region and a relatively strong warming to the south of it (Fig. 5a). By decomposing the response of the North Atlantic SST into the atmosphere-forced component driven by atmospheric forcing and the ocean-driven component induced by ocean circulation changes, we find that the atmosphere-forced component of the North Atlantic SST anomaly exhibits a relatively uniform warming across the entire basin, and thus does not contribute to the warming deficit in the WH region (Fig. 5b). On the contrary, the ocean-driven component shows an overall cooling of the North Atlantic basin, with the most pronounced cooling occurring in the WH region (Fig. 5c). In the WH region and Labrador Sea, the cooling driven by ocean circulation changes overwhelms the warming caused

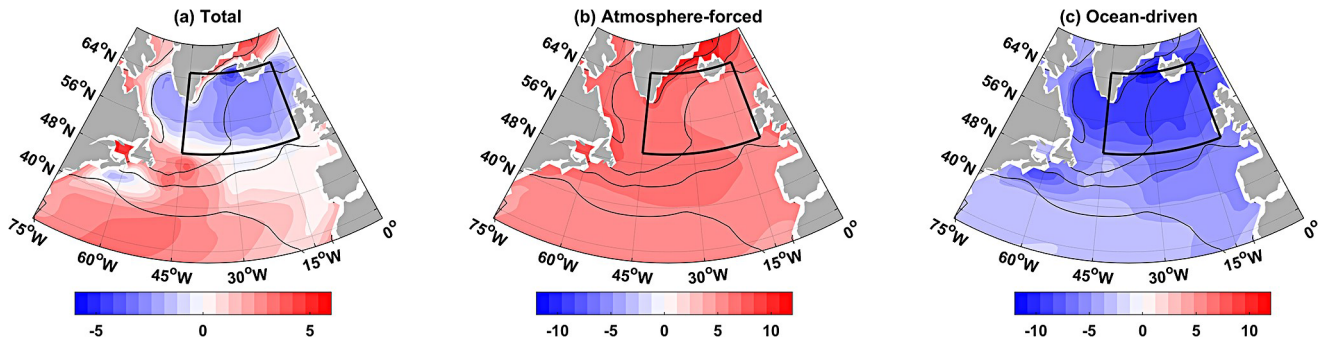

Fig. 5 Changes of SST (°C) over the subpolar North Atlantic in tour is the mean SST field in CTRL (CI = 5 °C). The box in each panel response to quadrupled CO_2: (**a**) the total response and its (**b**) atmo- indicates the WH region (45°W-10°W, 50°N-65°N) sphere-forced and (**c**) ocean-driven components. Superimposed con-

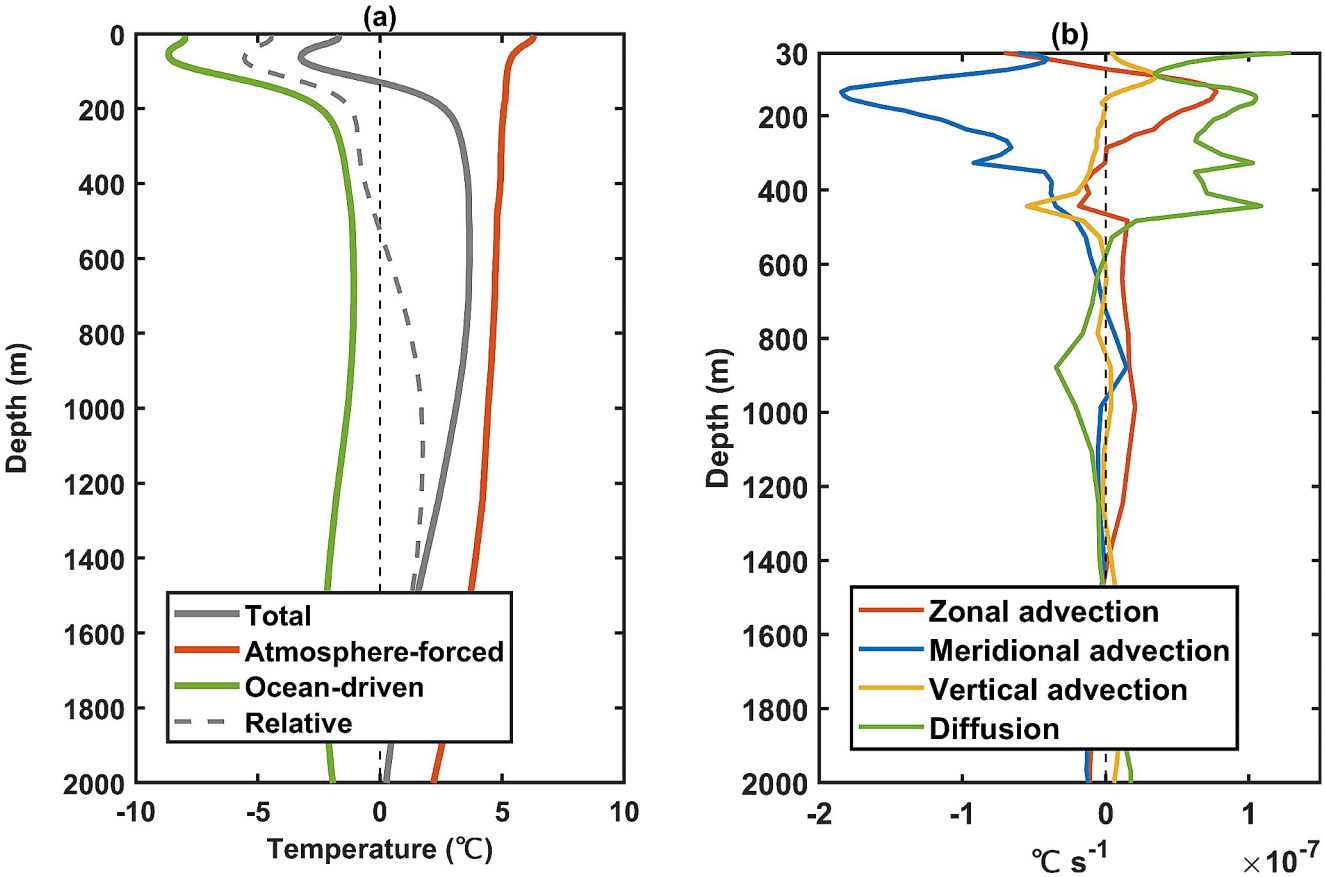

Fig. 6 (**a**) Vertical profiles of ocean temperature anomaly (°C) in the WH region in response to quadrupled CO_2: the total response (gray) and its atmosphere-forced (red) and ocean-driven (green) components. Superimposed dashed gray line is the relative ocean temperature anomaly between the WH region and the NH. (**b**) Vertical profiles of zonal (red), meridional (blue), vertical (yellow) advection and diffusion (green) anomalies (°C s^{-1}) in the WH region in response to quadrupled CO_2

by atmospheric forcing, while in other areas of the North Atlantic, the ocean-driven cooling is overcompensated by the atmosphere-forced warming. Quantitatively, the SST anomaly in the WH region is about − 0.9 °C in response to quadrupled CO_2, with the atmosphere-forced component contributing 6.3 °C and the ocean-driven component contributing − 7.2 °C. In conclusion, it is the ocean circulation changes that drive the spatial pattern of SST in the subpolar Atlantic (including the WH region) in response to quadrupled CO_2.

In addition to the spatial pattern of the WH, we also examine the vertical structure of the ocean temperature response averaged over the WH region (Fig. 6a). Results show that the ocean temperature in the WH region cools over the top ~ 135 m of the water column, with a peak at about 65 m (gray line in Fig. 6a), indicating that the WH is not driven by surface forcing. Furthermore, both the cooling over the top ~ 135 m and its peak are controlled by the ocean-driven component of the ocean temperature response (green line in Fig. 6a). The maximum cooling of ocean

temperature anomaly that occurs in the subsurface is consistent with the cooling effect of meridional advection (blue line in Fig. 6b) caused by the AMOC slowdown, which transports less warm water into this region from lower latitudes. The slowdown of the AMOC also reduces the downward penetration of the surface cooling signal through diffusion (green line in Fig. 6b), resulting in a rapid decay of the cooling with depth. The atmosphere-forced component of the ocean temperature response shows a warming throughout the entire water depth, with the strongest warming in the surface layer, and the warming tends to decrease with increasing depth (red line in Fig. 6a). When considering the relative changes in ocean temperature between the WH region and the NH, the relative cooling and warming occur above and below the depth of ~ 530 m (dashed gray line in Fig. 6a), a depth corresponding closely to the depth of the AMOC upper limb, which is defined as the mean depth of the maximum streamfunction. This finding is consistent with the result of Menary and Wood (2018) and indirectly supports the notion that the AMOC plays a significant role in the formation of the projected WH. Specifically, through a comparison of the relative changes in ocean temperature over WH region and depth of the AMOC across various CMIP5 models, Menary and Wood (2018) identified a close relationship between the vertical dipole structure of ocean temperature change and the depth of maximum streamfunction of AMOC. This occurs because the weakening AMOC leads to a decrease in the northward transport of warm water into the WH region in the upper layer, as well as a reduction in the downward transport of cold water.

We further examine the changes in surface heat flux (SHF) and its atmosphere-forced and ocean-driven components in the North Atlantic (Fig. 7). In response to quadrupled CO_2, the SHF anomaly in the North Atlantic is characterized by a large heat gain north of 40°N and a weak heat loss to the south (Fig. 7a). Specifically, there is a significant ocean heat gain in the Labrador Sea, WH region, and along the North American coast. The positive anomaly of the SHF in the northern North Atlantic is dominated by its ocean-driven component (comparing Fig. 7a with 7c), with a contribution from the atmosphere-forced component in the Labrador Sea and around Iceland (Fig. 7b). The atmosphere-forced component is relatively weak overall, indicating ocean heat loss in the center of the subpolar North Atlantic region (Fig. 7b). The widespread negative SST anomaly in the subpolar North Atlantic appears to contradict the strong positive SHF anomaly there (comparing Fig. 5a with 7a), which would have caused anomalous warming. Therefore, the presence of the WH there can only be explained by the dynamical role of the ocean, while the SHF works to compensate the dynamical cooling and establish a new equilibrium. This further verifies the critical role of ocean circulation changes in the formation of the WH. Furthermore, although the atmosphere-forced SHF response shows a negative anomaly in the center of the subpolar North Atlantic, the atmosphereforced SST response exhibits a relatively uniform warming across the entire basin (comparing Fig. 5b with 7b). This mismatch between the atmosphere-forced SHF and the SST response pattern arises from the advection of the temperature anomaly by the mean ocean circulation.

The SHF anomaly can be further decomposed into contributions from shortwave and longwave radiations, latent and sensible heat fluxes, and the heat flux due to sea ice formation and melt (Fig. 8). Results show that the contribution of the radiations is quite limited in both the atmosphere-forced and ocean-driven components. The positive SHF anomaly in the subpolar North Atlantic is dominated by its ocean-driven component and is primarily driven by a positive latent heat flux anomaly. A further decomposition of the latent heat flux change shows that the Newtonian

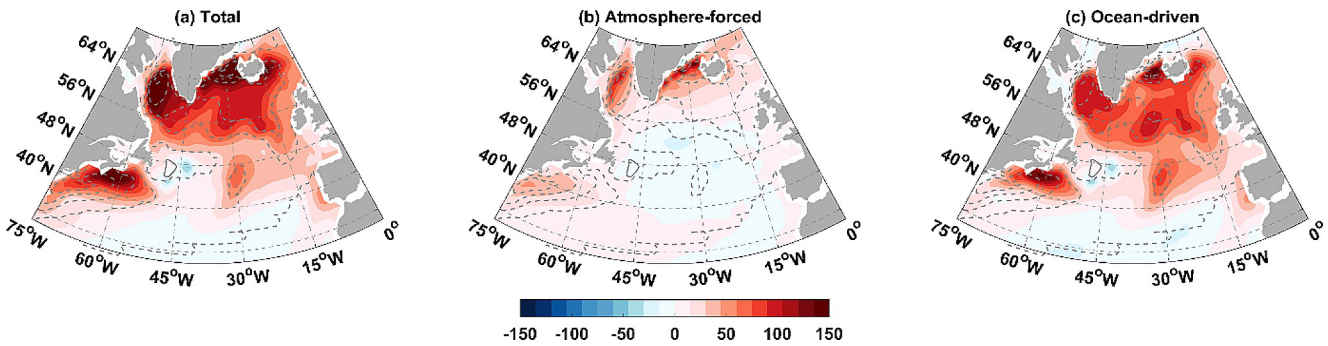

Fig. 7 Changes of the surface heat flux (SHF; positive into ocean; W ponents. Superimposed contour is the mean SHF in CTRL (solid and m^{-2}) over the North Atlantic in response to quadrupled CO_2: (**a**) the dashed lines for ocean heat gain and loss, respectively; CI = 50 W m^{-2}) total response and its (**b**) atmosphere-forced and (**c**) ocean-driven com-

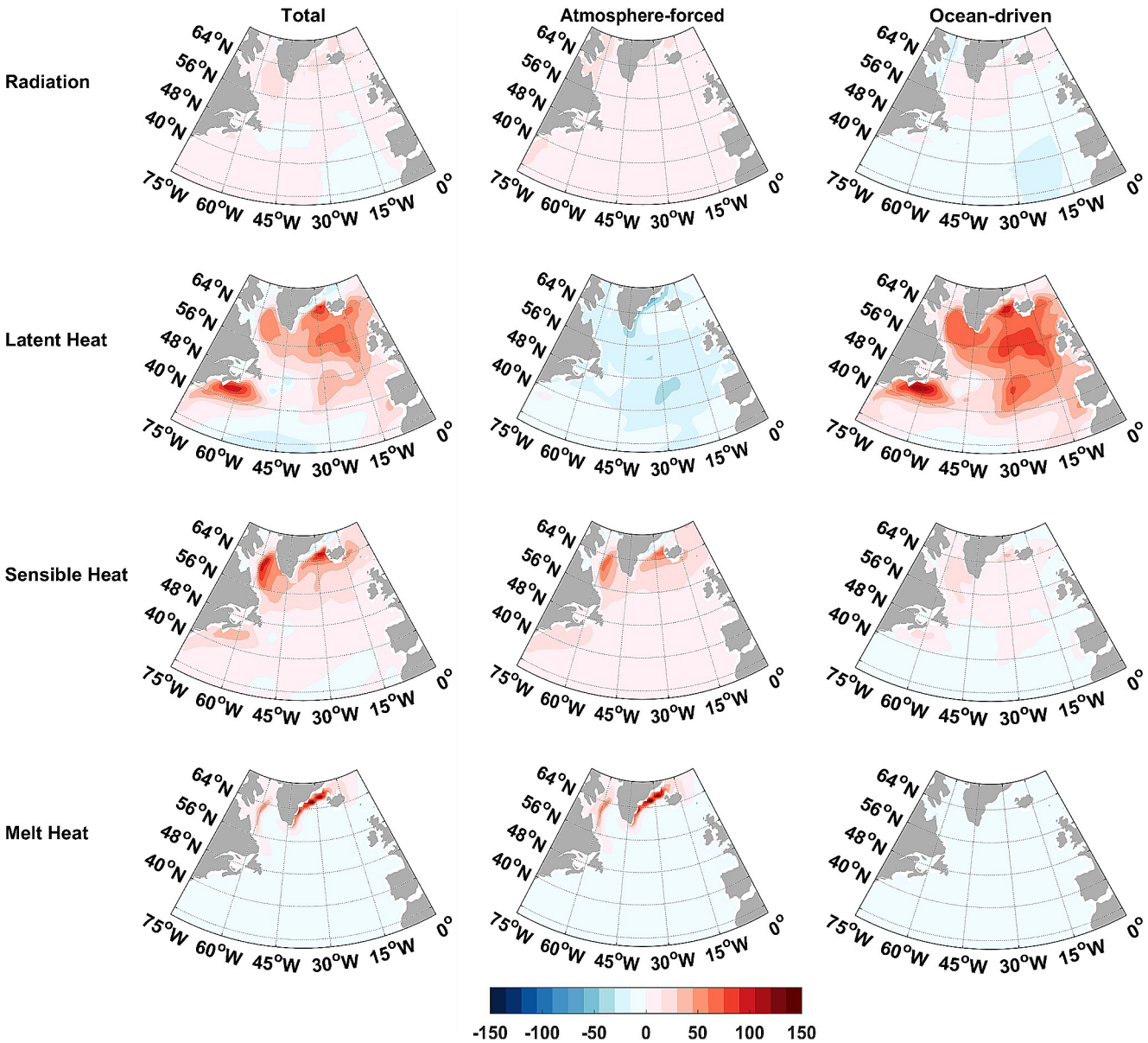

Fig. 8 Decomposition of the SHF anomalies (positive into the ocean; W m^{-2}) over the North Atlantic in response to quadrupled CO_2: shortwave and longwave radiations (first row), latent heat flux (second row), sensible heat flux (third row), and the heat flux due to sea ice formation and melt (forth row) in the total response (first column) and its atmosphere-forced (second column) and ocean-driven (third column) components

cooling effect associated with changes in SST dominates the positive anomaly, with the wind-evaporation-SST feedback also playing a role (not shown). To be specific, the slowdown of the AMOC leads to a reduction of the northward OHT and thus to a cooling of the SST in the WH region (Fig. 5c), causing the ocean to absorb more heat from the atmosphere through reducing the evaporative cooling on the SST. In addition, the ocean-driven component (positive) of the latent heat flux anomaly is partially offset by its atmosphere-forced component (negative). On the other hand, the atmosphere-forced component contributes positively to the positive SHF anomaly in the Labrador Sea and around Iceland, mainly through the sensible heat flux and the heat flux due to sea ice formation and melt.

In summary, the North Atlantic WH is predominantly driven by the changes in ocean circulation (i.e., the slowdown of the AMOC), and the contribution of atmospheric processes is negligible. As the AMOC slows down, the northward OHT across the North Atlantic decreases, resulting in a cooling of SST in the WH region, which further causes a positive downward SHF anomaly there. Previous studies have suggested that the weakening of the AMOC under greenhouse gas forcing is primarily due to increased SHF in the subpolar North Atlantic (Gregory et

al. 2005, 2016; Schmittner et al. 2005; Weaver et al. 2007; Cheng et al. 2013; Menary et al. 2013; Wen et al. 2018; Weijer et al. 2020; Couldrey et al. 2023). As more excess heat is absorbed by the ocean in the subpolar North Atlantic, the AMOC will slow down further. Therefore, there is a positive feedback from the ocean-driven SHF response in the subpolar North Atlantic to the initial AMOC weakening (Garuba and Klinger 2016; Gregory et al. 2016). This positive heat flux feedback will be discussed in detail in the next section.

4 Positive feedback mechanism in AMOC response

Previous studies have indicated that the ocean-driven SHF anomaly contributes to, and may even amplify, the slowdown of the AMOC, resulting in a positive feedback through the SHF (Garuba and Klinger 2016; Gregory et al. 2016). According to the experimental design, the partially coupled simulation considers only the influence of atmospheredriven SHF anomalies on the ocean circulation, while the fully coupled simulation takes into account the total SHF anomaly to force ocean circulation changes. Consequently, the difference between the fully coupled and partially coupled simulations can be exploited to isolate the effect of the SHF feedback on the AMOC change.

Figure 9 shows the temporal evolution of the AMOC strength changes in both the fully coupled and partially coupled simulations. It is evident that there are significant differences between the response of the AMOC in the two simulations. In the partially coupled simulation, the AMOC weakens rapidly and reaches a relatively stable state after approximately 20 years of simulation, resulting in a reduction of ~ 9 Sv after stabilization (red line in Fig. 9). On the other hand, in the fully coupled simulation, the AMOC continues to weaken beyond 20 years and stabilizes only after about 100 years, ultimately weakening by ~ 18 Sv (blue line in Fig. 9). As mentioned above, the difference in AMOC changes between these two simulations represents the role of the positive SHF feedback. Hence, the positive feedback through the SHF results in an AMOC weakening of ~ 9 Sv, which accounts for ~ 50% of the total weakening of the AMOC in response to quadrupled CO_2. This percentage is considerably higher than the 10% reported by Todd et al. (2020) in their comparison of coupled and ocean-only experiments. This finding suggests that previous studies might have underestimated the significance of this positive feedback through the SHF in the AMOC response to greenhouse gas forcing.

To further demonstrate the role of the positive feedback, we select four different time periods to compare the spatial patterns of AMOC response between the fully coupled and partially coupled simulations (Fig. 10). During the initial two decades, the AMOC response exhibits consistent AMOC weakening between the fully and partially coupled simulations, indicating an atmospheric source for the initial weakening (Fig. 10a and e). This corresponds to the rapid adjustment period of the ocean to the atmospheric forcing caused by increased CO_2. During this phase, the influence of the positive feedback through the SHF is weak and barely contributes to the AMOC response (Fig. 10i). However, as time goes on, the positive heat flux feedback becomes increasingly influential. Consequently, the AMOC weakening in the fully coupled simulation gradually surpasses that in the partially coupled simulation (compare Fig. 10b and

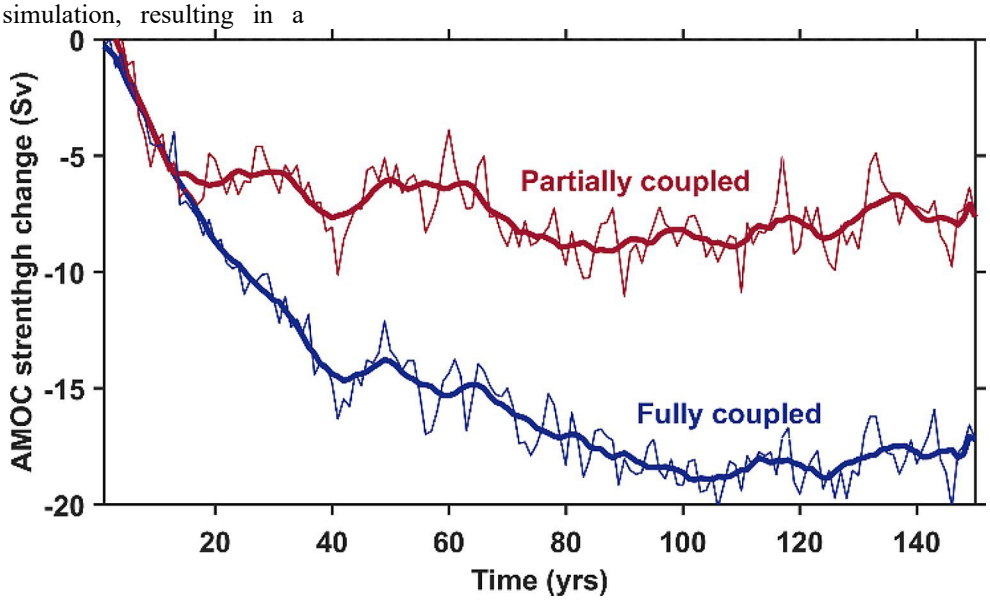

Fig. 9 Time series of AMOC strength changes (Sv) in the fully coupled (blue) and partially coupled (red) simulations in response to quadrupled CO_2. The AMOC strength is defined as the maximum streamfunction below 500 m at 45°N. Thin lines show annual means; thick lines are smoothed over 11 years

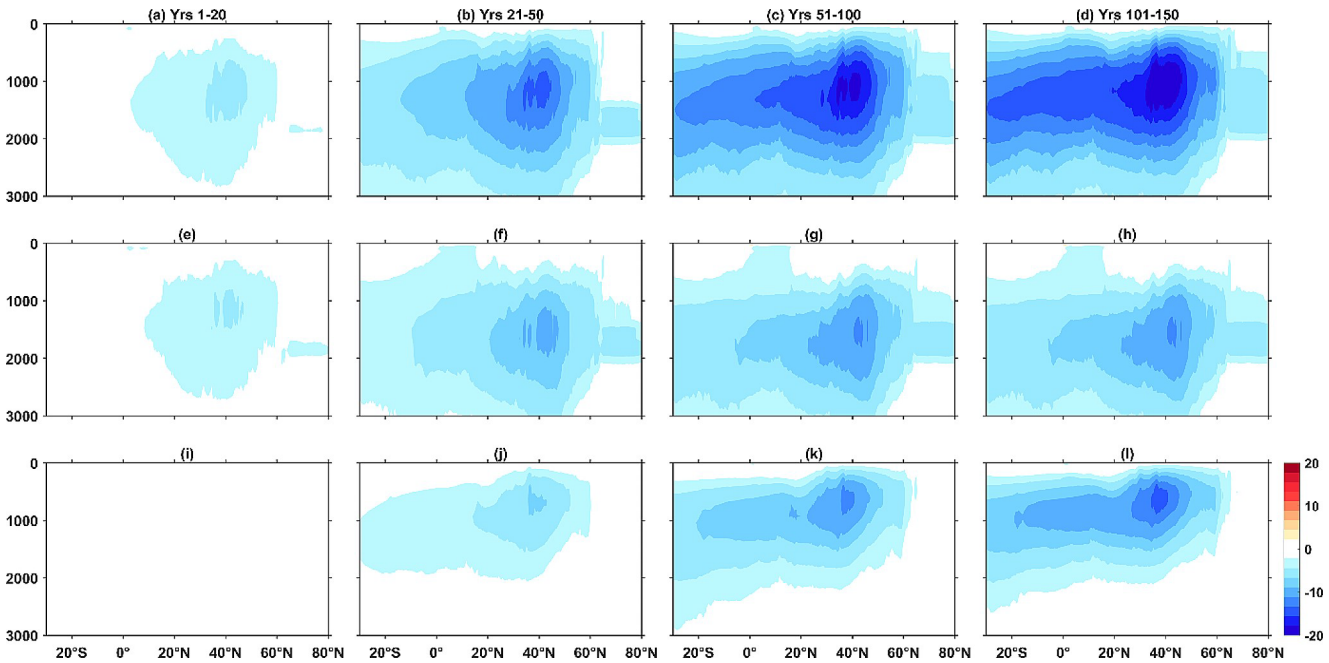

Fig. 10 The mean AMOC anomalies (Sv) in years 1 to 20 (first column), years 21 to 50 (second column), years 51 to 100 (third column) and years 101 to 150 (last column), in the fully coupled simulation (first row), partially coupled simulation (second row), and their differences (third row)

f). After ~ 20 years of simulation, the strength of the AMOC tends to stabilize and does not weaken further in the partially coupled simulation (Fig. 10f-h). In the fully coupled simulation, however, the AMOC continues to weaken due to the persistent influence of the positive feedback through the SHF (Fig. 10b-d). Therefore, the role of the positive feedback, as represented by the difference between the two simulations, becomes evident in weakening the AMOC after ~ 20 years of simulation (Fig. 10j-k). In addition, both the positive feedback through the SHF and the atmospheric forcing contribute comparably to the slowdown of the AMOC (compare Fig. 10h and l), with the former exerting a more pronounced impact on the shallower part of the AMOC.

Since the positive feedback results from the ocean-driven component of the SHF anomaly in the subpolar North Atlantic, here we further examine the temporal evolution of the changes in the SHF and its atmosphere-forced and oceandriven components (Fig. 11). The ocean-driven component is derived as the difference between the fully coupled and partially coupled simulations. During the initial two decades, the ocean-driven SHF anomaly remains quite weak, and the positive SHF anomaly in the subpolar North Atlantic is mainly controlled by its atmosphere-forced component (compare Fig. 11a and b). Simultaneously, the weakening of the AMOC during this period is predominantly driven by its atmosphere-forced component. Subsequently, the weakening of the AMOC leads to a negative SST anomaly in the subpolar North Atlantic through reduced northward OHT. This SST cooling, resulting from changes in ocean circulation, triggers a significant positive ocean-driven SHF anomaly over the same region (Fig. 11c). This effectively amplifies the excess heat absorbed by the ocean in the subpolar North Atlantic (Fig. 11a). The positive SHF anomaly induced by the AMOC weakening has also been shown in previous studies (Winton et al. 2013; Garuba and Klinger 2016; Gregory et al. 2016). The positive ocean-driven SHF anomaly plays an additional role in further weakening the AMOC. In other words, the weakening of the AMOC and the positive SHF anomaly in the subpolar North Atlantic reinforce each other, perpetuating the AMOC weakening.

In summary, the weakening of the AMOC during the initial two decades is forced by the atmosphere-driven SHF

anomaly, which represents the initial response. Subsequently, the SST cooling induced by the AMOC weakening provides feedback to the atmosphere-ocean interaction, resulting in a significant positive ocean-driven SHF anomaly over the subpolar North Atlantic. This positive ocean-driven SHF anomaly can further weaken the AMOC. This process reveals a positive feedback mechanism in the response of the AMOC in an atmosphere-ocean coupled system. The positive feedback acts to amplify the slowdown of the AMOC through adjusting the SHF anomaly in the subpolar North Atlantic. Quantitatively, this positive feedback through the SHF makes a substantial contribution, about 50%, to the overall weakening of the AMOC in response to quadrupled CO_2. This result underscores the key role of atmosphereocean coupling in determining how the AMOC responds to global warming.

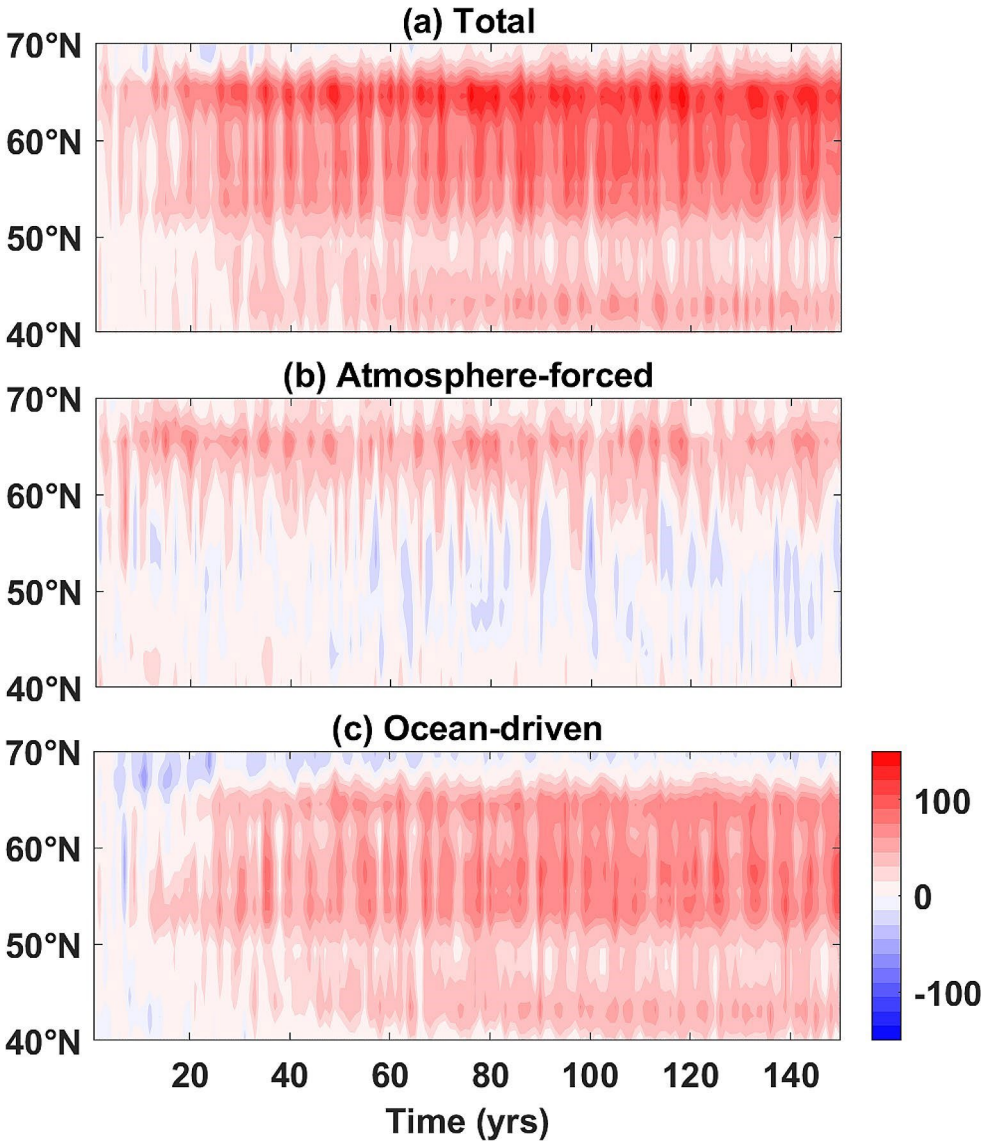

Fig. 11 Zonally averaged SHF anomalies (W m^{-2}) in the subpolar North Atlantic in (**a**) the total response and its (**b**) atmosphereforced and (**c**) ocean-driven components

5 Conclusion

This study investigates the mechanisms behind the formation of a projected North Atlantic WH under greenhouse gas forcing in the CESM model. Specifically, we aim to accurately verify the respective contributions of oceanic and atmospheric processes to the formation of the WH in response to quadrupled CO_2 in an atmosphere-ocean coupled system. With the help of a set of purposefully designed experiments in Garuba et al. (2018), we decompose the anomalous SST into two components: purely atmosphereforced (i.e., influenced by atmospheric processes) and ocean-driven (i.e., driven by changes in ocean circulation). Furthermore, we explore the impact of a positive coupled feedback through the SHF on the AMOC response under greenhouse gas forcing within this self-consistent framework. The main conclusions of this study are as follows:

Firstly, the crucial role of the AMOC slowdown in the projected WH under greenhouse gas forcing is confirmed by the results of the purposefully designed experiments. In response to quadrupled CO_2, the change of SST in the subpolar North Atlantic is consistently weaker than that in the NH, a phenomenon known as the North Atlantic WH. Through isolating the active ocean dynamical response, we find that the temporal evolution of the WH is predominantly ocean-driven, and the contribution of atmospheric processes is negligible. This is consistent with previous studies, which found that oceanic processes dominate the projected WH (Woollings et al. 2012; Rugenstein et al. 2013; Winton et al. 2013; Marshall et al. 2015; Gervais et al. 2018; Menary and Wood 2018; Chemke et al. 2020; Keil et al. 2020; Liu et al. 2020; Ren and Liu 2021). To be specific, since the AMOC is responsible for transporting warm water from the equatorial regions to the subpolar North Atlantic, when the AMOC weakens, there is a reduced transport of warm water to the subpolar region, resulting in a cooling of SST there. The spatial pattern and the vertical structure of the ocean temperature response in the WH region also confirm that the WH is not driven by a surface forcing but by the AMOC weakening. In addition, the cooling of SST in the subpolar North Atlantic corresponds to a strong positive SHF anomaly there, indicating that the effect of the SHF works to compensate for the SST cooling. The positive SHF anomaly in the subpolar North Atlantic is dominated by the oceandriven component, which is mainly driven by the positive latent heat flux anomaly there.

Another major finding of this study is that there is a positive feedback through the SHF in the response of the AMOC under greenhouse gas forcing in the coupled atmosphereocean system. In particular, atmospheric forcing initially leads to a weakening of the AMOC, which in turn leads to a negative SST anomaly in the subpolar North Atlantic through a reduced northward OHT. This ocean-driven SST cooling results in a significant positive SHF anomaly in the subpolar North Atlantic, which further contributes to the ongoing weakening of the AMOC. This positive feedback through the SHF has also been shown in previous studies (Garuba and Klinger 2016; Gregory et al. 2016; Tood et al. 2020). However, this study goes a step further and quantifies the role of the positive feedback in the AMOC response through numerically isolating the ocean-dynamics induced SHF in a more realistic framework. We find that the positive feedback through the SHF acts to double the weakening of the AMOC from ~ 9 Sv in the partially coupled simulation to ~ 18 Sv in the fully coupled simulation. Thus, this positive feedback mechanism through the SHF has important implications for our understanding of the AMOC response, as well as the model uncertainty in the AMOC weakening under greenhouse gas forcing.

It is important to acknowledge several limitations of this study. Firstly, we rely on a single model for our analysis. The relative roles of oceanic and atmospheric processes in the formation of the WH, as well as the influence of the positive coupled feedback on the AMOC response, may vary between different climate models. Further investigations with diverse models are needed to determine the robustness of our results. Moreover, the CESM model, although valuable, may not fully capture all processes of the real ocean-atmosphere-sea ice system. For example, the current version of CESM lacks an active Greenland ice sheet component, which could have a significant impact on both the timing and strength of WH formation (Gervais et al. 2018). Ongoing efforts to improve the model physics will be necessary to increase our confidence in the simulation results.

Acknowledgements We acknowledge Dr. Oluwayemi Garuba for sharing the data of the fully and partially coupled experiments with tracers. This work is supported by the National Natural Science Foundation of China (NSFC; 42230405) and the Laoshan Laboratory (No. LSKJ202202401). This research used resources of the National Energy Research Scientific Computing Center (NERSC), a U.S. Department of Energy Office of Science User Facility located at Lawrence Berkeley National Laboratory, operated under Contract No. DE-AC02-05CH11231 using NERSC award ERCAP0017151. J. L. is supported by the U.S. Department of Energy Office of Science Biological and Environmental Research as part of the Regional and Global Model Analysis program area. Pacific Northwest National Laboratory is operated for DOE by Battelle Memorial Institute under contract DE-AC05-76RL01830. F. L. is supported by the "Youth Innovation Team Program" Team in Colleges and Universities of Shandong Province (No. 2022KJ042) and Fundamental Research Funds for the Central Universities (No. 202341016).

Author contributions Y. Luo, J. Lu and F. Liu were responsible for design of the research. The first draft of the manuscript was written by Q. Li and all authors commented on previous versions of the manuscript. All authors read and approved the final manuscript.

Funding This work is supported by the National Natural Science Foundation of China (NSFC; 42230405) and the Laoshan Laboratory (No. LSKJ202202401).

Data availability The CESM data used in this study are available from the corresponding author upon request.

Declarations

Competing interests The authors have no relevant financial or nonfinancial interests to disclose.

References

Bakker P, Schmittner A, Lenaerts JTM, Abe-Ouchi A, Bi D, van den Broeke MR, Yin J (2016) Fate of the Atlantic Meridional overturning circulation: strong decline under continued warming and Greenland melting. Geophys Res Lett 43(23) 12,252 – 12,260. https://doi.org/10.1002/2016GL070457.

Banks HT, Gregory JM (2006) Mechanisms of ocean heat uptake in a coupled climate model and the implications for tracer based

predictions of ocean heat uptake. Geophys Res Lett 33(7):3–6. https://doi.org/10.1029/2005GL025352.

Bouttes N, Gregory JM, Kuhlbrodt T, Smith RS (2014) The drivers of projected North Atlantic sea level change. Clim Dyn 43(5–6):1531–1544

Caesar L, Rahmstorf S, Robinson A, Feulner G, Saba V (2018) Observed fingerprint of a weakening Atlantic Ocean overturning circulation. Nature 556(7700):191–196. https://doi.org/10.1038/s41586-018-0006-5.

Chemke R, Zanna L, Polvani LM (2020) Identifying a human signal in the North Atlantic warming hole. Nat Commun 11(1):1–7. https:// doi.org/10.1038/s41467-020-15285-x.

Cheng W, Chiang JCH, Zhang D (2013) Atlantic meridional overturning circulation (AMOC) in CMIP5 models: RCP and historical simulations. J Clim 26(18):7187–7197. https://doi.org/10.1175/ JCLI-D-12-00496.1.

Collins M et al (2013) Long-term climate change: Projections, commitments and irreversibility, in *Climate Change 2013: The Physical Science Basis. Contribution of Working Group I to the Fifth Assessment Report of the Intergovernmental Panel on Climate Change*, edited by T. Stocker., pp. 1029–1136, Cambridge Univ.
Press, Cambridge, U. K., and New York, https://doi.org/10.1017/CBO9781107415324.024.

Couldrey MP, Gregory JM, Dong X et al (2023) Greenhouse-gas forced changes in the Atlantic meridional overturning circulation and related worldwide sea-level change. Clim Dynamic 60:2003–2039. https://doi.org/10.1007/s00382-022-06386-y.

Dagan G, Stier P, Watson-Parris D (2020) Aerosol Forcing Masks and delays the formation of the North Atlantic warming hole by three decades. Geophys Res Lett 47(22):1–10. https://doi.org/10.1029/2020GL090778.

Drijfhout S, van Oldenborgh GJ, Cimatoribus A (2012) Is a decline of AMOC causing the warming hole above the North Atlantic in observed and modeled warming patterns? J Clim 25(24):8373–8379. https://doi.org/10.1175/JCLI-D-12-00490.1.

Garuba OA, Klinger BA (2016) Ocean heat uptake and interbasin transport of the passive and redistributive components of surface heating. J Clim 29(20):7507–7527. https://doi.org/10.1175/ JCLI-D-16-0138.1.

Garuba OA, Rasch PJ (2020) A partial coupling method to isolate the roles of the atmosphere and Ocean in coupled climate simulations. J Adv Model Earth Syst 12(9). https://doi.org/10.1029/2019MS002016.

Garuba OA, Lu J, Liu F, Singh HA (2018) The active role of the Ocean in the temporal evolution of Climate Sensitivity. Geophys Res Lett 45(1):306–315. https://doi.org/10.1002/2017GL075633.

Gervais M, Atallah E, Gyakum JR, Tremblay B, L (2016) Arctic air masses in a warming world. J Clim 29(7):2359–2373. https://doi.org/10.1175/JCLI-D-15-0499.1.

Gervais M, Shaman J, Kushnir Y (2018) Mechanisms governing the development of the North Atlantic Warming Hole in the CESMLE future climate simulations. J Clim 31(15):5927–5946. https://doi.org/10.1175/JCLI-D-17-0635.1.

Gervais M, Shaman J, Kushnir Y (2019) Impacts of the North Atlantic warming hole in future climate projections: Mean atmospheric circulation and the North Atlantic jet. J Clim 32(10):2673–2689. https://doi.org/10.1175/JCLI-D-18-0647.1.

Gregory JM, Dixon KW, Stouffer RJ, Weaver AJ, Driesschaert E, Eby M, Thorpe RB (2005) A model intercomparison of changes in the Atlantic thermohaline circulation in response to increasing atmospheric CO_2 concentration. Geophys Res Lett 32(12):1–5. https:// doi.org/10.1029/2005GL023209.

Gregory JM, Bouttes N, Griffies SM, Haak H, Hurlin WJ, Jungclaus J, Kelley M, Lee WG, Marshall J, Romanou A, Saenko OA, Stammer D, Winton M (2016) The flux-anomaly-forced Model Intercomparison Project (FAFMIP) contribution to CMIP6: investigation of sea-level and ocean climate change in response to CO2 forcing. Geosci Model Dev 9(11):3993–4017. https://doi.org/10.5194/gmd-9-3993-2016.

Haarsma RJ, Selten FM, Drijfhout SS (2015) Decelerating Atlantic meridional overturning circulation main cause of future west European summer atmospheric circulation changes. Environ Res Lett 10(9). https://doi.org/10.1088/1748-9326/10/9/094007.

Haney RL (1971) Surface Thermal Boundary Condition for Ocean circulation models. J Phys Oceanogr 1(4):241–248. https://doi.org/10.1175/1520-0485(1971)001%3C0241:STBCFO%3E2.0.CO;2.

He C, Clement AC, Cane MA, Murphy LN, Klavans JM, Fenske TM (2022) A north atlantic warming hole without ocean circulation. Geophys Res Lett 49(19):1–11. https://doi.org/10.1029/2022GL100420.

Hu S, Fedorov Av (2020) Indian Ocean warming as a driver of the North Atlantic warming hole. Nat Commun 11(1):1–11. https://doi.org/10.1038/s41467-020-18522-5.

IPCC (2021) Summary for Policymakers. In: Climate Change 2021: The Physical Science Basis. Contribution of Working Group I to the Sixth Assessment Report of the Intergovernmental Panel on Climate Change [Masson-Delmotte, V., P. Zhai, A. Pirani, S. L. Connors, C. Péan, S. Berger, N. Caud, Y. Chen, L. Goldfarb, M. I. Gomis, M. Huang, K. Leitzell, E. Lonnoy, J.B.R. Matthews, T. K. Maycock, T. Waterfield, O. Yelekçi, R. Yu and B. Zhou (eds.)]. Cambridge University Press. In Press. Retrieved from https://www.ipcc.ch/report/ar6/wg1/.

Keil P, Mauritsen T, Jungclaus J, Hedemann C, Olonscheck D, Ghosh R (2020) Multiple drivers of the North Atlantic warming hole. Nat Clim Change 10(7):667–671. https://doi.org/10.1038/ s41558-020-0819-8.

Kim H, An S, Il (2013) On the subarctic North Atlantic cooling due to global warming. Theoret Appl Climatol 114(1–2):9–19. https://doi.org/10.1007/s00704-012-0805-9.

Li L, Lozier MS, Li F (2022a) Century-long cooling trend in subpolar North Atlantic forced by atmosphere: an alternative explanation. Clim Dyn 58(9–10):2249–2267. https://doi.org/10.1007/ s00382-021-06003-4.

Li Q, Luo Y, Lu J, Liu F (2022b) The role of Ocean Circulation in Southern Ocean Heat Uptake, Transport, and Storage response to quadrupled CO2. J Clim 35(22):7165–7182. https://doi.org/10.1175/JCLI-D-22-0160.1.

Liu W, Fedorov AV, Xie SP, Hu S (2020) Climate impacts of a weakened Atlantic meridional overturning circulation in a warming climate. Sci Adv 6(26):1–9. https://doi.org/10.1126/sciadv.aaz4876.

Ma X, Liu W, Burls NJ, Chen C, Cheng J, Huang G, Li X (2021) Evolving AMOC multidecadal variability under different CO2 forcings. Clim Dyn 57(1–2):593–610. https://doi.org/10.1007/s00382-021-05730-y.

Marshall J, Scott JR, Armour KC, Campin JM, Kelley M, Romanou A (2015) The ocean's role in the transient response of climate to abrupt greenhouse gas forcing. Clim Dyn 44(7–8):2287–2299. https://doi.org/10.1007/s00382-014-2308-0.

Menary MB, Wood RA (2018) An anatomy of the projected North Atlantic warming hole in CMIP5 models. Clim Dyn 50(7–8):3063–3080. https://doi.org/10.1007/s00382-017-3793-8.

Menary MB, Roberts CD, Palmer MD, Halloran PR, Jackson L, Wood RA, Lee SK (2013) Mechanisms of aerosol-forced AMOC variability in a state of the art climate model. J Geophys Research:

Oceans 118(4):2087–2096. https://doi.org/10.1002/jgrc.20178.
Rahmstorf S, Willebrand J (1995) The role of temperature feedback in stabilizing the Thermohaline circulation. J Phys Oceanogr 25(5):787–805. https://doi.org/10.1175/1520-0485(1995)025%3C0787:TR OTFI%3E2.0.CO;2.
Rahmstorf S, Box JE, Feulner G, Mann ME, Robinson A, Rutherford S, Schaffernicht EJ (2015) Exceptional twentieth-century slowdown in Atlantic Ocean overturning circulation. Nat Clim Change 5(5):475–480. https://doi.org/10.1038/nclimate2554.
Ren X, Liu W (2021) The role of a weakened Atlantic Meridional Overturning Circulation in modulating Marine heatwaves in a warming climate. Geophys Res Lett 48(23):1–9. https://doi.org/10.1029/2021GL095941.
Rugenstein MAA, Winton M, Stouffer RJ, Griffies SM, Hallberg R (2013) Northern High-Latitude Heat Budget Decomposition and transient warming. J Clim 26(2):609–621. https://doi.org/10.1175/JCLI-D-11-00695.1.
Schmittner A, Latif M, Schneider B (2005) Model projections of the North Atlantic thermohaline circulation for the 21st century assessed by observations. Geophys Res Lett 32(23):1–4. https://doi.org/10.1029/2005GL024368.
Todd A, Zanna L, Couldrey M, Gregory J, Wu Q, Church JA et al (2020) Ocean-only FAFMIP: understanding regional patterns of ocean heat content and dynamic sea level change. J Adv Model Earth Syst 12:e2019MS002027. https://doi.org/10.1029/2019MS002027
Weaver AJ, Eby M, Kienast M, Saenko OA (2007) Response of the Atlantic meridional overturning circulation to increasing atmospheric CO2: sensitivity to mean climate state. Geophys Res Lett 34(5):1–5. https://doi.org/10.1029/2006GL028756.
Weaver AJ, Sedláček J, Eby M, Alexander K, Crespin E, Fichefet T, Zickfeld K (2012) Stability of the Atlantic meridional overturning circulation: a model intercomparison. Geophys Res Lett 39(20):1–7. https://doi.org/10.1029/2012GL053763.
Weijer W, Cheng W, Garuba OA, Hu A, Nadiga BT (2020) CMIP6 models predict significant 21st century decline of the Atlantic Meridional overturning circulation. Geophys Res Lett 47(12). https://doi.org/10.1029/2019GL086075.
Wen Q, Yao J, Döös K, Yang H (2018) Decoding hosing and heating effects on global temperature and meridional circulations in a warming climate. J Clim 31(23):9605–9623. https://doi.org/10.1175/JCLI-D-18-0297.1.
Winton M, Griffies SM, Samuels BL, Sarmiento JL, Licher TLF (2013) Connecting changing ocean circulation with changing climate. J Clim 26(7):2268–2278. https://doi.org/10.1175/ Woollings T, Gregory JM, Pinto JG, Reyers M, Brayshaw DJ (2012) Response of the North Atlantic storm track to climate change shaped by ocean-atmosphere coupling. Nat Geosci 5(5):313–317. https://doi.org/10.1038/ngeo1438.
Xie P, Vallis GK (2012) The passive and active nature of ocean heat uptake in idealized climate change experiments. Clim Dyn 38(3–4):667–684. https://doi.org/10.1007/s00382-011-1063-8.